Infrared Phys. Vol. 29, No. 2-4, pp. 541–549, 1989
Printed in Great Britain.

0020-0891/89 $3.00 + 0.00

ULTRAHIGH RESOLUTION FAR-INFRARED SPECTROSCOPY OF METHANOL

G. MORUZZI
Dipartimento di Fisica dell'Università di Pisa, Pisa, Italy

M. PREVEDELLI
Scuola Normale Superiore, Pisa, Italy

K. M. EVENSON, D. A. JENNINGS, M. D. VANEK
National Bureau of Standards, Boulder, CO 80303, USA

and

M. INGUSCIO
Dipartimento di Scienze Fisiche dell'Università di Napoli, Napoli, Italy

(Received 17 September 1988)

Abstract—Seventy-eight absorption lines, located in an extremely crowded portion of the CH_3OH spectrum, have been measured with a tunable coherent FIR spectrometer, based on third order mixing in a point contact diode. The high experimental resolution (20 kHz) allows the separation of overlapping lines observed with a Fourier transform spectrometer. Comparisons with previous Fourier transform measurements and theoretical predictions are presented. A separate measurement reveals that the 170 μm laser line of CH_3OH is very close to a strong absorption line, possibly explaining the peculiar Stark behavior of the laser line and a large reported apparent pressure shift.

1. INTRODUCTION

Tunable far-infared (TuFIR) radiation has been generated with several different techniques:[1,2] harmonics of microwave oscillators, difference frequency generation of CO_2 lasers in GaAs, difference frequency mixing of a far-infrared (FIR) laser and microwave radiation, and difference generation in a metal–insulator–metal diode from a pair of CO_2 lasers. The latter technique, used in the present study, has proven to be an extremely valuable tool for the measurement of highly accurate FIR spectra. The frequencies of the stable species are used as frequency and wavelength calibration standards, and the high resolution of the method is useful in the study of molecular line broadening, line shift, and line shape parameters.

Tunability is obtained either by using a waveguide CO_2 laser with about ± 120 MHz tunability for one of the CO_2 lasers (i.e. in second order), or by adding microwave sidebands to the CO_2 laser frequency difference (i.e. in third order). The third order technique used in the present work offers a much wider FIR spectral coverage from each CO_2 line pair. By selecting appropriate pairs of CO_2 lines, this technique permits the coverage of the complete FIR spectral region with an accuracy of ± 50 kHz.

The high resolution of this technique makes it particularly well suited for the investigation of the most crowded portions of complex molecular spectra, where instrumentally caused line overlapping occurs with spectrometers using wavelength rather than frequency techniques (for instance, Fourier transform spectrometers).

An interesting case is the CH_3OH molecule, in which Fourier Transform measurements, covering the 8–300 cm^{-1}[3–6] and 700–1100 cm^{-1}[7] spectral regions, have been made. There are several small intervals (their widths are of the order of a few hundredths wavenumbers) where severe line overlaps occur due to the lack of sufficient FTS resolution. The use of the TuFIR technique, with its Doppler limited high resolution (an improvement of about 2 orders of magnitude with respect to FTS), has led to the resolution of most of the lines to be described.

2. THE METHANOL SPECTRUM

The methanol spectrum has been the subject of much theoretical and experimental investigation since 1939.[8,9] At first, the interest was mainly of a theoretical nature, because CH_3OH is one of the most complicated 6 atom molecules, and it presents several interesting problems for an appropriate quantum mechanical description. The introduction of the optically pumped molecular lasers[10] has added a strong practical interest to the spectroscopy of methanol. In fact, CH_3OH is the richest and most efficient known laser active molecule in the FIR region, with more than 400 lasing lines between 30 μm and 2 mm. Its isotopic species are also laser-active, and, for instance, CD_3OH is known to lase at more than 300 FIR frequencies. The practical interest for the spectroscopy of all the isotopic species of methanol is dramatically increased by the fact that these molecules, together with CH_2F_2, are the only available rich laser sources between 2 and 8 THz.[11] The desire to assign the known laser lines and the possibility of predicting new possible laser emissions are at the origin of systematic investigations of the methanol spectrum, which include the FT spectra mentioned in the introduction. Up to now, more than 14000 FIR and infrared absorption lines of methanol have been assigned.[3-7]

The CH_3OH Hamiltonian has been described, and particularly extensive and clear treatments have been presented by Lees and Baker[12] and by Kwan and Dennison.[13] Here we shall confine ourselves to a brief summary. The energy levels are labeled by 6 quantum numbers corresponding to the symmetry species, the vibrational state, the torsional state, and the usual angular momentum quantum numbers J, K and M: $|Sy, v, n, J, K, M>$. The symmetry species for methanol are A, E_1, and E_2. A 6 atom molecule has $(6 \times 3) - 6 = 12$ normal vibrational modes; in the case of CH_3OH one of these corresponds to the internal hindered rotation (torsion) of the OH and CH_3 groups with respect to each other. Simultaneous excitation of two or more of the remaining 11 pure vibrational modes is usually not observed in absorption FIR spectra. For each of these vibrational modes, usually only the ground and first excited states are observed. Most of the observed lasing transitions occur within the first excited level of the C–O stretch vibrational mode, in this case the v label is usually written "CO", whereas the v label is written "0" for the ground vibrational state (no pure vibrations excited). Lasing transitions involving OH-bend, CH_3 deformation, CH_3 rocking and other vibrational modes have also been observed.[14,15] As stated above, the quantum number n describes the torsion, J is the total angular momentum, K and M are the J components along the methyl axis and along a laboratory fixed direction, respectively. As long as no external field is applied there is complete degeneracy over M, and this quantum number is omitted in the labels. Because of the asymmetry of the molecule, only J and the symmetry are rigorously good quantum numbers. The selection rules for electric dipole transitions are $\Delta J = 0, \pm 1$, $\Delta K = 0, \pm 1$, Δn and Δv any; however, $\Delta K = 0$ is allowed only if $\Delta n = 0$, and only $\Delta K = 0$ is allowed if the C–O stretch state is changed in the transition. Transitions are allowed only within the same symmetry species.

There is a degeneracy between the $|E_1, v, n, J, K>$ and $|E_2, v, n, J, -K>$ states which cannot be resolved because the Hamiltonian has no matrix elements connecting states belonging to different symmetries; however, the degeneracy between $|A, v, n, J, K>$ and $|A, v, n, J, -K>$ is resolved and gives origin to a K doubling as in the case of a rigid asymmetric top. An additional label, + or − according to the convention by Ivash and Dennison,[12,16] is added in order to distinguish between the members of a doublet. The splitting between the members of a K doubling pair increases with increasing J, but decreases dramatically with increasing K. For example, the determination of the splitting coefficient for $K = 6$ has only been possible by means of TuFIR spectroscopy.[9] The K doubling of states belonging to A-type symmetry with $K > 6$ has not been experimentally observed up to now.

The methanol absorption spectrum is extremely crowded and scattered over the spectral region between the microwave and about 1200 cm^{-1} because of two principal reasons: (i) the selection rules allow $\Delta K = \pm 1$ transitions (which are forbidden for symmetric top molecules), and (ii) the three main contributions to the energy of the levels, i.e. overall rotation, torsion and pure vibrations, are successively higher in frequency: the rotational constant B is approximately 0.8 cm^{-1}, the height of the torsional barrier is of the order of 370 cm^{-1} and the frequencies of the lowest pure vibrational modes are of the order of 1000 cm^{-1}. As an example of the richness and density of the methanol spectrum, 40,000 absorption lines have been counted in a FT spectrum

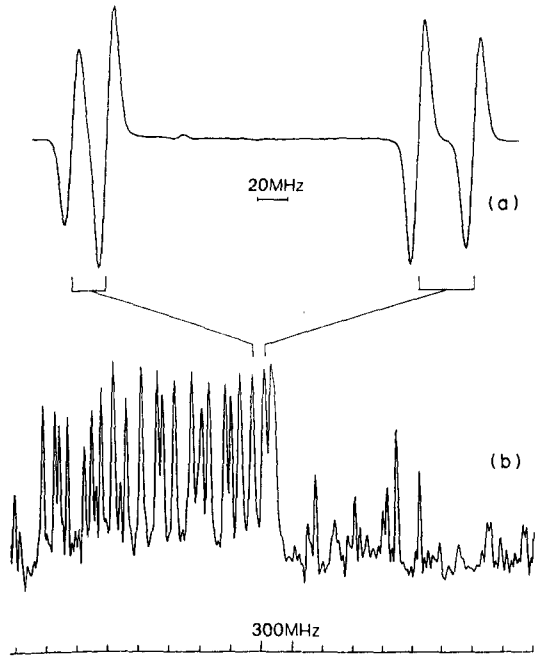

Fig. 1. Comparison of the resolutions of a FT (b) and a TuFIR (a) spectrometer. The line structure in the left half of (a) is the $|E_2\,0, 2, 1, J> \leftarrow |E_2, 0, 1, 2, J>$ Q-branch. Two single peaks of (b) are seen to be actually doublets in (a).

between 30 and 206 cm^{-1} by the authors of Refs (3–6). Thus, although the already assigned 14,000 lines might seem a huge amount, the larger part of the assignment work is still waiting to be done. Under these conditions, many line overlappings within the FTS resolution occur. This makes the use of TuFIR spectroscpy of particular relevance for the investigation of the methanol spectrum. On the other hand, this spectrum is spread over such a wide region that, even with the increased spectral coverage of the third order TuFIR spectrometer, it would take over one thousand scans to cover it completely. Thus, the combined use of both experimental techniques, TuFIR and FT spectroscopy, is convenient for the investigation of the methanol and other similar crowded spectra.

3. EXPERIMENTAL DETAILS

The third order TuFIR spectrometer has been described previously:[18] here, we shall briefly review its essential features. Each CO_2 laser is stabilized to a CO_2 sub-Doppler saturated fluorescence feature using separate low pressure cells, the uncertainty of the lock is 25 kHz. The overall uncertainty in the FIR frequency is thus of the order of 35 kHz. The two laser emissions are mixed, together with the microwaves generated by a Klystron in a metal–insulator–metal diode. The diode is formed by a tungsten whisker contacting a naturally oxidized cobalt base. In order to minimize FIR amplitude noise and maintain bolometer sensitivity, the FIR radiation is frequency modulated. A frequency modulation up to 3 MHz at a one kilohertz rate is obtained by frequency modulating the CO_2 lasers by means of piezoelectric drivers on the end mirrors. The FIR detectors and the lock-in amplifier detect at the modulation rate, as a consequence, the recorded signal is the derivative of the absorption signal.

As an example of the resolution achieved, Fig. 1 shows the $|\text{Sym}, v, n, K, J>:|E_2\ 0, 2, 1, J> \leftarrow |E_2, 0, 1, 2, J>$ Q-branch, where two pairs of collapsed lines of the FT spectrum[15](b) are clearly resolved in the TuFIR spectrum (a). The fact that the two observed FTS single lines were actually doublets had already been pedicted by the computer fit of the FT spectrum with the correct assignments given in Table 1.

Table 1 reports the absorption frequencies recorded using the 9P(16) line of $^{12}C^{16}O_2$ (31491437.3923 MHz) and the 10R(28) line of $^{13}C^{16}O_2$ (27997038.9638 MHz) as CO_2 laser lines with the microwaves swept from 5 to 10 GHz. For Table 2 the 9P(18) line of $^{12}C^{16}O_2$

Table 1. Lower and upper sideband absorption frequencies recorded using the 9P(16) line of $^{12}C^{16}O_2$ (31491437.3923 MHz) and the 10R(28) line of $^{13}C^{16}O_2$ (31438060.1801 MHz) with the microwaves swept from 5 to 10 GHz. The TuFIR frequencies and the available assignments are reported and compared to the FT measurements and to the frequencies evaluated by a computer best fit program starting from the FT spectrum. Lines overlapping in the FT spectrum are marked by an asterisk

TuFIR (cm^{-1})	Sym	Assignment $(n'K'J') \leftarrow (n''K''J'')$	FT obs.	FT calc. (cm^{-1})	(cm^{-1})	Overlap
		Lower sideband				
116.2298612	E_2	Q(2, 1; 17) ← (1, 2; 17)		116.23264	116.23110	*
	E_2	Q(2, 1; 18) ← (1, 2; 18)		116.23264	116.23203	*
	E_2	Q(2, 1; 16) ← (1, 2; 16)		116.23264	116.23330	*
116.2370127	E_2	Q(2, 1; 19) ← (1, 2; 19)		116.23748	116.23661	*
116.2382134	E_2	Q(2, 1; 15) ← (1, 2; 15)		116.23748	116.23812	*
116.2451561	E_2	Q(2, 1; 14) ← (1, 2; 14)		116.24548	116.24507	*
116.2459391	E_2	Q(2, 1; 20) ← (1, 2; 20)		116.24548	116.24540	*
	E_2	Q(2, 1; 13) ← (1, 2; 13)		116.25374	116.25369	*
	E_1	R(2, 5; 9) ← (2, 6; 8)		116.25374	116.25512	*
116.2596679	E_2	Q(2, 1; 21) ← (1, 2; 21)		116.25967	116.25894	
116.2635830	E_2	Q(2, 1; 12) ← (1, 2; 12)		116.26345	116.26354	
116.2742842	E_2	Q(2, 1; 11) ← (1, 2; 11)		116.27425	116.27420	
116.2788257	E_2	Q(2, 1; 22) ← (1, 2; 22)		116.27901	116.27780	
116.2854030	E_2	Q(2, 1; 10) ← (1, 2; 10)		116.28528	116.28532	
116.2966262	E_2	Q(2, 1; 9) ← (1, 2; 9)		116.29640	116.29652	
116.3040388	E_2	Q(2, 1; 23) ← (1, 2; 23)		116.30425	116.30254	
116.3076406	E_2	Q(2, 1; 8) ← (1, 2; 8)		116.30751	116.30751	
116.3181330	E_2	Q(2, 1; 7) ← (1, 2; 7)		116.31808	116.31799	
116.3279468	E_2	Q(2, 1; 6) ← (1, 2; 6)		116.32788	116.32771	
116.3358291				116.33642		*
116.3367688	E_2	Q(2, 1; 5) ← (1, 2; 5)		116.33642	116.33646	*
116.3443379	E_2	Q(2, 1; 4) ← (1, 2; 4)		116.34426	116.34403	
116.3506020	E_2	Q(2, 1; 3) ← (1, 2; 3)		116.35055	116.35028	
116.3554567	E_2	Q(2, 1; 2) ← (1, 2; 2)		116.35532	116.35507	
	E_2	P(1, 3; 27) ← (0, 4; 28)		116.36643	116.36648	
116.3717956	E_2	Q(2, 1; 25) ← (1, 2; 25)		116.37190	116.37181	*
116.3723176				116.37190		*
116.3749277				116.37484		
116.3825490	E_2	P(2, 0; 14) ← (2, 1; 15)		116.38278	116.38261	
		Upper sideband				
116.6181303				116.61953		
116.6385931				116.63852		
116.6429258				116.64312		
116.6870355				116.68704		
116.6908462				116.69076		
116.7013908				116.70138		
116.7248290	E_2	R(1, 14; 17) ← (0, 15; 16)		116.72491	116.72306	
116.7453962				116.74523		
116.7904978				116.79044		
116.7972840				116.79747		
116.8027129				116.80252		

(31438060.1801 MHz) and the 10P(32) line of $^{13}C^{16}O_2$ (26563453.0887 MHz) have been used. Both tables report both the lower and upper sideband measurements and the comparison with the FT results of Ref. (5). The lower sideband of Table 1 covers the $|E_2, 0, 2, 1, J> \leftarrow |E_2, 0, 1, 2, J>$ Q-branch, and the upper sideband of Table 2 covers the $|E_2, 0, 2, 6, J> \leftarrow |E_2, 0, 2, 5, J>$ Q-branch and, partially, the $|E_2, 0, 1, 3, J> \leftarrow |E_2, 0, 0, 4, J>$ Q-branch.

A minor problem in the interpretation of the TuFIR spectra is the overlapping of the lower and upper sideband resonances. In fact, assuming a frequency difference $\Delta\omega$ between the CO_2 lasers, a resonance signal at the microwave frequency $\delta\omega$ may correspond to an actual absorption frequency either at $\Delta\omega + \delta\omega$ or at $\Delta\omega - \delta\omega$. However the two cases are recognizable from the signal by the shape, the negative part of the signal coming first for the $\Delta\omega + \delta\omega$ resonances, and the positive part coming first for the $\Delta w - \delta\omega$ resonances. Moreover, if the same spectral region can signal by the shape, the negative part of the signal coming first for the $\Delta\omega + \delta\omega$ resonances, and the positive part coming first for the $\Delta w - \delta\omega$ resonances. Moreover, if the same spectral region can be covered starting from a different CO_2 pair, a shift of the lower and upper sideband resonances with respect to each other is observed in the two measurements, as is shown in Fig. 3.

4. EXPERIMENTAL RESULTS AND DISCUSSION

Several dozen absorption lines have been measured with high accuracy, and we have been able to assign many of them. The measured frequencies, the available assignments and a comparison

Table 2. Lower and upper sideband absorption frequencies recorded using the 9P(18) line of $^{12}C^{16}O_2$ (31438060.1801 MHz) and the 10P(32) line of $^{13}C^{16}O_2$ (26563453.0887 MHz) with the microwaves swept from 5 to 10 GHz. The TuFIR frequencies and the available assignments are reported and compared to the FT measurements and to the frequencies evaluated by a computer best fit program starting from the FT spectrum. Lines overlapping in the FT spectrum are marked by an asterisk

TuFIR (cm^{-1})	Sym	Assignment $(n'K'J') \leftarrow (n''K''J'')$	FT obs.	FT calc. (cm^{-1})	(cm^{-1})	Overlap
		Lower sideband				
162.1465704				162.14660		
162.1687036				162.16874		
162.1871827				162.18964		*
162.1893230				162.18964		*
162.2054530	E_2	Q(1, 3; 20) ← (0, 4; 20)		162.20547	162.20592	
162.2083241				162.20866		
162.2301441				162.22987		
162.2560880				162.25608		
162.2621955				162.26224		
162.2757155				162.27559		
162.2831803				162.28320		
162.3601245				162.36010		*
162.3623691				162.36010		*
162.3884174	E_2	Q(2, 3; 18) ← (0, 4; 18)		162.38834	162.38810	
		Upper sideband				
162.8087081	E_2	Q(1, 3; 12) ← (0, 4; 12)		162.80900	162.80853	
162.8132456	E_2	Q(2, 6; 26) ← (2, 5; 26)		162.81313	162.81341	
162.8305830	E_2	Q(2, 6; 25) ← (2, 5; 25)		162.83109	162.83055	
162.8466060	E_2	Q(2, 6; 24) ← (2, 5; 24)		162.84606	162.84638	
162.8526614				162.85246		
162.8613789	E_2	Q(2, 6; 23) ← (2, 5; 23)		162.86135	162.86106	*
	E_2	Q(1, 3; 11) ← (0, 4; 11)		162.86135	162.86120	*
162.8753166	E_2	Q(2, 6; 22) ← (2, 5; 22)		162.87524	162.87470	
162.8880536	E_2	Q(2, 6; 21) ← (2, 5; 21)		162.88815	162.88738	
	E_2	Q(2, 6; 20) ← (2, 4; 20)		162.90031	162.89917	
	E_2	Q(1, 3; 10) ← (0, 4; 10)		162.90956	162.90915	*
162.9106044	E_2	Q(2, 6; 19) ← (2, 5; 19)		162.90956	162.91010	*
162.9206270	E_2	Q(2, 6; 18) ← (2, 5; 18)		162.92078	162.92021	
	E_1	R(1, 8; 21) ← (0, 9; 20)		162.92979	162.92893	*
162.9297622	E_2	Q(2, 6; 17) ← (2, 5; 17)		162.92979	162.92953	*
162.9381143	E_2	Q(2, 6; 16) ← (2, 5; 16)		162.93817	162.93807	
162.9457356	E_2	Q(2, 6; 15) ← (2, 5; 15)		162.94591	162.94587	
	E_2	Q(1, 3; 9) ← (0, 4; 9)		162.95259	162.95245	*
162.9525740	E_2	Q(2, 6; 14) ← (2, 5; 14)		162.95259	162.95296	*
162.9589425	E_2	Q(2, 6; 13) ← (2, 5; 13)		162.95908	162.95934	
162.9646324	E_2	Q(2, 6; 12) ← (2, 5; 12)		162.96515	162.96506	*
	E_2	R(2, 0; 14) ← (2, 1; 13)		162.96515	162.96774	*
162.9698003	E_2	Q(2, 6; 11) ← (2, 5; 11)		162.96937	162.97015	
162.9743418	E_2	Q(2, 6; 10) ← (2, 5; 10)		162.97452	162.97563	
162.9784135	E_2	Q(2, 6; 9) ← (2, 5; 9)		162.97854	162.97856	
162.9819631	E_2	Q(2, 6; 8) ← (2, 5; 8)		162.98212	162.98195	
	A	R(2, 4; 7) ← (1, 3; 6)		162.98505	162.98457	*
162.9851474	E_2	Q(2, 6; 7) ← (2, 5; 7)		162.98505	162.98485	*
162.9878096				162.98809		
162.9910983	E_2	Q(1, 3; 8) ← (0, 4; 8)		162.99116	162.99119	
162.9993460				162.99929		
163.0176686				163.01773		
163.0253421	E_2	Q(1, 3; 7) ← (0, 4; 7)		163.02519	163.02544	*
	A	R(2, 6; 33) ← (2, 7; 32)		163.02519	163.02603	*
163.0454395				163.04566		
163.0490413				163.04909		
163.0550967	E_2	Q(1, 3; 6) ← (0, 4; 6)		163.05500	163.05526	

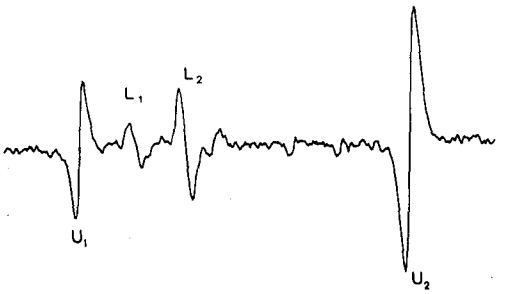

Fig. 2. Lower (L) and upper (U) sideband resonances. Both resonances are measured simultaneously and are superposed in the microwave scan. However, they are recognizable from each other, since the negative part of the signal occurs first in the upper sideband resonances, last in the lower sideband resonances. The wavenumbers of the lines recorded in the figure are L_1: 162.3623691 cm^{-1}, L_2: 162.3601245 cm^{-1}, U_1: 162.8466060 cm^{-1} and U_2: 162.8613789 cm^{-1}.

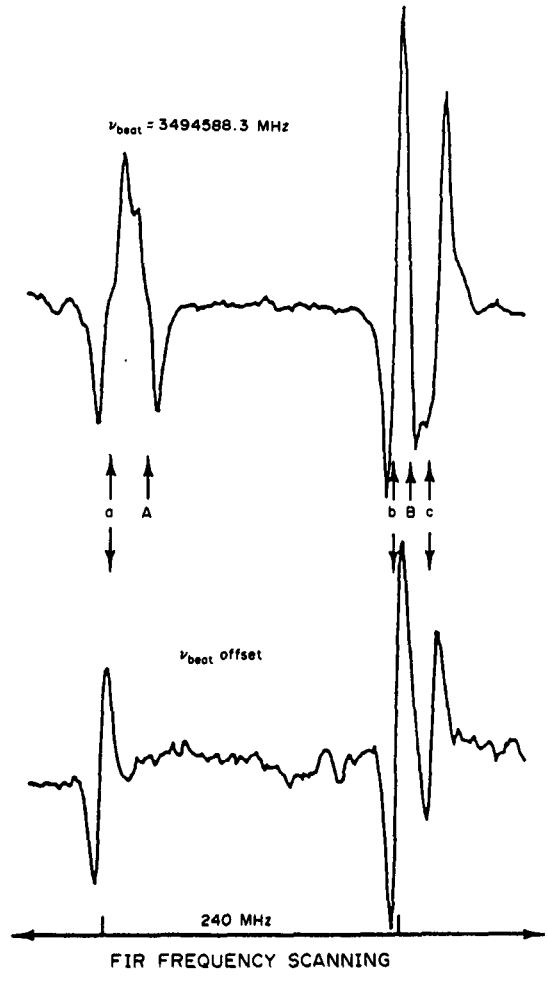

Fig. 3. Resonances originating from the lower and upper microwave sidebands can be shifted with respect to each other by covering the same spectral region starting from a different CO_2 pair. The lower sideband resonances denoted by the upper case letters A and B in the upper recording are absent from the lower recording.

with the corresponding FT measurements, as well as with the frequencies evaluated by a computer best fit program starting from the FT spectrum, are shown in Tables 1 and 2. The columns marked FT and fit data are from Ref. (5). It is interesting to note that, while the agreement between TuFIR and FT measurements is always within the experimental errors, the agreement between the TuFIR measurements and the fit frequencies is usually better, often by almost an order of magnitude. This is expected because the fit contains a whole series of lines, and the information contained in all the lines is used for the evaluation of each single frequency. Thus, as mentioned in the preceding section, the fit program is able to predict that some lines observed as single in the FT spectrum actually correspond to different transitions which overlap within the FT resolution. The overlapping lines are marked by asterisks in Tables 1 and 2. Actually, the fit program also shows that a TuFIR line of Table 1 and 7 TuFIR lines of Table 2 correspond to superpositions of separate transitions within the TuFIR spectrometer resolution. The superposition is seen as a distortion of the signal in the experimental recordings. The 116.230 cm^{-1} line is predicted by the theory to correspond to three separate transitions and is shown in Fig. 4. The fit program follows line series by expanding the energies of levels sharing all the quantum numbers but J into Taylor series in $J(J+1)$

$$E(q,J) = \sum_{m=0} a_m(q)[J(J+1)]^m \pm \frac{1}{2}\frac{(J+K)!}{(J-K)!}[S(K) + J(J+1)T(K)], \tag{1}$$

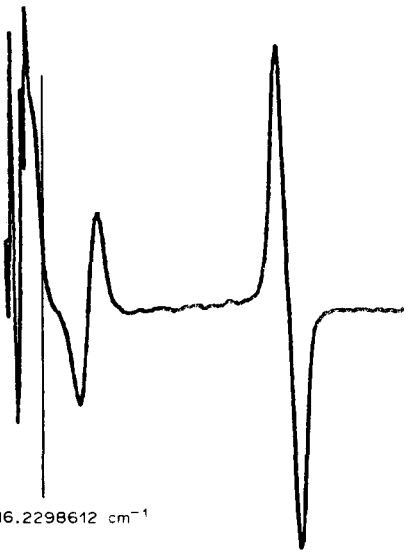

Fig. 4. The TuFIR signal at 116.2298612 cm^{-1} actually corresponds to three overlapping transitions: $|E_2, 0, 2, 1; 17> \leftarrow |E_2, 0, 1, 2; 17>$, $|E_2, 0, 2, 1; 18> \leftarrow |E_2, 0, 1, 2; 18>$, $|E_2, 0, 2, 1; 16> \leftarrow |E_2, 0, 1, 2; 16>$. This superposition occurs within the TuFIR resolution, its presence, however, is shown by the deformation of the signal.

which usually can be truncated at $m = 4$ ($m = 3$ is always needed, whereas one never needs $m > 5$). q stands for the set of all the residual quantum numbers, the term in S and T describes the K doubling and is needed only for A-type symmetry levels with $0 < K \leqslant 6$. When different line series are followed, or when a Q-branch bends onto itself, as in the cases of Tables 1 and 2, the program can often predict two or more overlapping lines (i.e. that a single experimental signal must correspond to more than one transition in order to complete the line series). But, for instance, the TuFIR signal of Fig. 4 shows that the spread of the three overlapping lines is probably somewhat smaller than predicted by the fit program.

When dealing with overlapping lines, one should remember that the origin of the overlappings found in a molecular spectrum can be twofold: either (i) casual coincidences or near coincidences of lines belonging to unrelated line series, or of lines belonging to a same series but with otherwise unrelated quantum numbers (for instance, when a Q-branch bends onto itself); or (ii) the lines are doublets. In the first, the lines can often be resolved without the use of TuFIR. As we have already discussed, the computer fit of a line series increases the accuracy on the frequencies of the single lines, and, more important, it can predict the occurrence of two or more lines at the same location. In this case TuFIR can confirm that the fit program has run correctly (or that no perturbation, which could not be treated by the computer program, affects the line series); it also increases the accuracy by at least one further order of magnitude. It should also be remembered that an overlapping of this kind is also possible between two lines belonging to line series, at least one of which has not yet been identified, as in the case of the 170 μm laser line which we shall discuss below. In this case, of course, a computer fit program cannot resolve the doublet and the use of TuFIR spectroscopy offers the only possibility of discovering a doublet. In the case of doublet (or triplet etc) structures, TuFIR can be essential for the resolution. When a whole line series, for instance, is affected by an asymmetry doubling smaller than the FTS resolution, there is no computational way to resolve the doublets starting from a FT spectrum. In such a situation, the TuFIR technique allows the determination of the asymmetry splitting constant of the $K = 6$ levels of the ground vibrational, ground torsional, A-type symmetry state of CH_3OH.[17]

A last interesting application of the TuFIR spectroscopy, which actually is a subcase of case (i), originates from the possibility of observing laser lines in absorption spectra (both FT and TuFIR). These lines display a lower intensity since their lower level is scarcely populated. A relevant case is represented by the CH_3OH 170 μm laser line, mentioned above, which has been found to lie very close to a yet unassigned absorption line (Fig. 5). The lines are so close that they could not be resolved by FTS. The unassigned absorption line corresponds to a transition between two levels

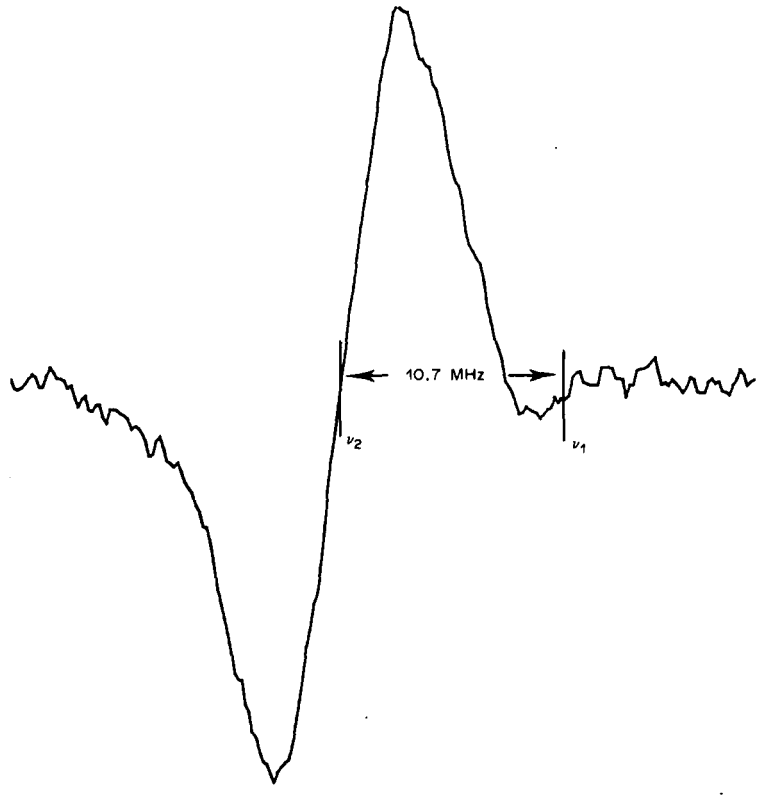

Fig. 5. TuFIR absorption spectrum of CH_3OH around the 170 μm laser line ν_1 (frequency: 1757526.3 MHz). The vapor pressure is 18 Pa. The absorption corresponding to the laser line appears weaker because its lower level is in the excited vibrational state. The frequency of the nearby strong absorption line ν_2 is 1757537.054 MHz. The frequency of the 170 μm lasing lines is thus only 10.7 MHz different from ν_2, and this can explain its behavior in the presence of electric fields.

of the ground vibrational state, as is clearly seen from its high intensity. Although the laser line is assigned, it would have been practically impossible to follow the weak line series it belongs to in an FT absorption spectrum. Thus, there was no possibility of resolving this overlapping in the FTS by a computer program. In this case, TuFIR spectroscopy has again been essential. This casual overlapping is extremely interesting. In fact, it can explain the peculiar Stark behavior of the 170 μm laser line ($|$Sym, v, n, K; $J>$:$|E_1$, CO, O, 8; 16$>\leftarrow|E_1$, CO, 7; 16$>$) which dies out very rapidly at very low values of an applied external electric field. This power decrease has been a puzzle for a long time because it is much faster than is observed for any other CH_3OH laser line. According to the quantum numbers involved in the transition, such a dramatic Stark effect is not to be expected[19,20] This behavior can now be explained if we assume that the nearby absorption line is shifted into resonance with the laser line by the electric field. This would imply that low J values are involved in the unassigned absorption line.[19]

This casual near overlapping of the 170 μm laser line with a strong absorption line might also explain the otherwise nonunderstandable pressure shift measured for this laser line by Lawandy *et al.*,[21,22] in contrast with other measurements[23] and theoretical calculations[24] on the same line, which lead to a much smaller pressure shift. It would be interesting to investigate if the overlapping can play a rôle in Lawandy's experimental situation.

5. CONCLUSIONS

The high resolution of TuFIR spectroscopy permits the separation of molecular lines which are not resolved with lower resolution methods. This feature is extremely important for the investigation of complicated molecular spectra like methanol where the high spectral density makes casual line overlapping probable, and where line structures due to such effects as very small asymmetry doublings are present. TuFIR spectroscopy has also shown that the CH_3OH 170 μm

laser line lies in very close proximity to an unassigned absorption line. This near resonance can explain the peculiar Stark behavior of this laser line, which dies out when even very weak electric fields are applied; this is in contrast to the quantum mechanical prediction that the laser line itself should not be affected.

Acknowledgement—One of the authors (M.P.) gratefully acknowledges a grant from the European Laboratory for Nonlinear Spectroscopy (LENS), Florence.

REFERENCES

1. K. M. Evenson, D. A. Jennings and F. R. Petersen, *Appl. Phys. Lett.* **44,** 576 (1984).
2. K. M. Evenson, D. A. Jennings, K. R. Leopold and L. R. Zink. *Laser Spectroscopy VII, Proc. 7th Int. Conf. Hawaii.* Springer, Berlin (1985).
3. G. Moruzzi, F. Strumia, C. Bonetti, B. Carli, F. Mencaraglia, M. Carlotti, G.Di Lonardo and A. Trombetti, *J. molec. Spectrosc.* **105,** 24 (1984).
4. G. Moruzzi, F. Strumia, P. Carnesecchi, B. Carli and M. Carlotti, *Infrared Phys.* **29,** 47 (1989).
5. G. Moruzzi, F. Strumia, P. Carnesecchi, B. Carli, M. Carlotti, R. M. Lees and I. Mukhopadhyay, In preparation.
6. G. Moruzzi, F. Strumia, P. Carnesecchi, R. M. Lees, I. Mukhopadhyay and M. Winnewisser, In preparation.
7. L. Coudert and A. Valentin, *J. molec. Spectrosc.* **122,** 390 (1987).
8. A. Borden and E. F. Barker, *J. chem. Phys.* **6,** 553 (1939).
9. J. S. Koehler and D. M. Dennison, *Phys. Rev.* **57,** 1006 (1940).
10. T. Y. Chang and T. J. Bridge, *Opt. Commun.* **1,** 423 (1970).
11. M. Inguscio, G. Moruzzi, K. M. Evenson and D. A. Jennings, *J. appl. Phys.* **60,** R161 (1986).
12. R. M. Lees and J. G. Baker, *J. chem. Phys.* **48,** 5299 (1968).
13. Y Y. Kwan and D. M. Dennison, *J. molec. Spectrosc.* **43,** 291 (1972).
14. J. O. Henningsen, *Int. J. infrared millimeter Waves,* **7,** 1605 (1986).
15. I. Mukhopadhyay, R. M. Lees and J. W. C. Johns, *J. appl. phys.* In press.
16. E. V. Ivash and D. M. Dennison, *J. chem. Phys.* **21,** 1804 (1953).
17. L. R. Zink, K. M. Evenson, D. A. Jennings, G. Moruzzi and M. Inguscio: *J. molec. Spectrosc.* **127,** 44 (1988).
18. K. M. Evenson, D. A. Jennings, L. R. Zink and K. R. Leopold, *Digest 11th Int. Conf. Infrared and Millimeter Waves,* Tirrenia-Pisa (Edited by G. Moruzzi). ETS, Pisa (1986).
19. M. Inguscio, A. Moretti, G. Moruzzi and F. Strumia, *Int. J. infrared millimeter Waves* **2,** 943 (1981).
20. F. Strumia and M. Inguscio, In: *Infrared and Millimeter Waves,* vol. 5, part I, p. 129 (Edited by K. J. Button). Academic Press, New York (1982).
21. N. W. Lawandy and G. A. Koepf, *Opt. Lett.* **5,** 383 (1980).
22. N. W. Lawandy, G. A. Koepf and D. L. McFarlane; *Infrared Phys.* **25,** 751 (1985).
23. M. Inguscio and K. M. Evenson; *Opt. Lett.* **9,** 443 (1984).
24. G. Buffa, G. Moruzzi and O. Tarrini, *Infrared Phys.* **27,** 349 (1987).